Available online at www.sciencedirect.com
ScienceDirect
Bioorganic & Medicinal Chemistry 16 (2008) 2591–2605
Bioorganic & Medicinal Chemistry

Activity of Mannich bases of 7-hydroxycoumarin against Flaviviridae

Mauro Mazzei,[a,*] Erika Nieddu,[a] Mariangela Miele,[a] Alessandro Balbi,[a] Marco Ferrone,[b] Maurizio Fermeglia,[b] Marco T. Mazzei,[b,†] Sabrina Pricl,[b] Paolo La Colla,[c] Fabio Marongiu,[c] Cristina Ibba[c] and Roberta Loddo[c]

[a]*Department of Pharmaceutical Sciences, Viale Benedetto XV, 3, 16132 Genova, Italy*
[b]*Molecular Simulation Engineering (MOSE) Laboratory, Department of Chemical Engineering, Piazzale Europa 1, 34127 Trieste, Italy*
[c]*Department of Biomedical Sciences and Technologies, University of Cagliari, Cittadella Universitaria, 09042 Monserrato, Cagliari, Italy*

Received 12 September 2007; revised 12 November 2007; accepted 16 November 2007

Abstract—Some Mannich bases of 7-hydroxycoumarin (**2**) and their simple derivatives (**3** and **4**) were prepared and tested against viruses containing single-stranded, positive-sense RNA genomes (ssRNA$^+$). This study was directed toward Flaviviridae and, in particular, HCV surrogate viruses (BVDV, YFV). The 7-hydroxy derivatives **2** were generally devoid of activity, but when position 7 was propylated, the resulting 7-propyloxy derivatives **3** were in some cases endowed with an interesting activity against BVDV. The formation of 7-benzoyl derivatives **4** gave compounds generally lacking in activity against Flaviviridae, whereas the appearance of activity against RSV has been observed. Also some unsymmetrical methylene derivatives **5**–**7** (namely coumarins bridged to chromones or indoles) were found moderately active in antiviral tests. Derivatives **3** were submitted to a molecular modeling study using DNA polymerase of HCV as a target. The good correlation between calculated molecular modeling IC_{50} and experimental EC_{50} indicates that DNA polymerase is potentially involved in the inhibition of surrogate HCV viruses.

1. Introduction

Hepatitis C is a widespread viral disease caused by hepatitis C virus (HCV), a virus belonging to the Flaviviridae family. The pathologic state may remain dormant for many years and when the disease becomes evident, the liver has already suffered severe damage, potentially leading to a chronic infection. Such chronic hepatitis may finally turn into hepatocarcinoma.[1–4]

Up to now, the only management of the disease was treatment with ribavirin and IFN-α.[5] The use of pegilated IFN-α has led to a drug giving weekly protection.[6] As these drugs have little efficacy in a large percentage of patients, the search for more active drugs is of extreme interest and relevance. Up to now, this search has been hampered by the lack of an efficient cell culture system. This impediment has recently been overcome by the development of subgenomic HCV RNA molecules that replicate autonomously in transfected cells.[7] Actually, some research groups have reported the development of a robust HCV infection system, which could facilitate future in vitro experiments.[8,9] Otherwise, as in the present study, the biological tests must be performed on viruses (namely BVDV, YFV, Dengue) similar to HCV.

After the unveiling of the HCV genoma, several sites of the viral genoma have been identified as targets for HCV drugs.[10–13] The major targets are internal ribosome entry site (IRES), non-structural proteins NS3 (with protease-elicase activity) and NS5B (with RNA-dependent RNA polymerase activity). With regards to this, many nucleoside analogs were found to bind specifically to viral targets.[14,15] Also, non-nucleoside inhibitors are the

Keywords: Antiviral agents; Flaviviridae; HCV; Mannich bases; Coumarin derivatives.
* Corresponding author. Tel.: +39 010 3538371; fax: +39 010 3538358; e-mail: mauro.mazzei@unige.it
† Present address: DIMES—Viale Benedetto XV, 1-16132 Genova, Italy.

0968-0896/$ - see front matter © 2007 Elsevier Ltd. All rights reserved.
doi:10.1016/j.bmc.2007.11.045

objective of vigorous research for anti-HCV drugs. Such inhibitors also include, besides drug-like molecules,[16–19] peptidomimetics[20,21] and oligonucleotides.[22]

Following our interest in benzopyrans,[23–25] this paper is devoted to exploring the activity of some Mannich bases of 7-hydroxycoumarin (**2**) and their simple derivatives in position 7 as *n*-propyl ethers (**3**) and benzoyl esters (**4**) against Flaviviridae. It is well known that natural and synthetic coumarins have multiple biological activities.[26] For instance, they have been claimed to be useful as anticoagulant, antibacterial, antiinflammatory, anticancer, and anti-HIV agents.[27–30] Very few are reported to be able to counteract HCV. As far as we know, only some coumarin derivatives present in patents and Osthole (7-methoxy-8-prenylcoumarin) are capable of inhibiting HCV replication and/or proliferation.[31,32] In particular, Osthole is able to counteract the progression of hepatitis C into hepatocarcinoma.[33] The action of Osthole causes a strong reduction of plasma alanine aminotransferase and also inhibits caspase-3 activation.[34] Osthole derivatives exhibiting more solubility in water in respect to the parent compound were recently proposed as hepatoprotective drugs.[35] For the biological action of Osthole, the presence of methoxy group is essential: in fact, the 7-hydroxy derivative, Osthenol, is devoid of activity.[33]

Since the great variability of pharmacological response of coumarins is connected to large modifications of their substituents, we found it interesting to synthesize some coumarin Mannich bases in order to examine their ability to inhibit HCV replication. This idea proved to be a winning strategy: in fact, a number of synthesized compounds showed moderate but significant activity against Flaviviridae family, paving the way for new coumarins to be used in hepatitis C virus infections.

Although this work was specifically targeted toward finding non-nucleoside drugs active against surrogate HCV viruses, the Mannich bases **2**–**4** were also tested against CVB-2, Sb-1, RSV, VSV, VV, Reo, HIV viruses.

Some unsymmetrical methylene derivatives (**5**–**7**), related to the above Mannich bases and already synthesized in previous works,[25,36] were also tested to verify their possible activity against HCV-related viruses as well as a panel of other viruses.

2. Chemistry

The Mannich bases **2a**–**q**, starting from 7-hydroxycoumarins **1** with 40% formaldehyde and suitable secondary amines in 95% ethanol, were prepared to form the title compounds. The hydroxy group in position 7 was in turn propylated or benzoylated (see Scheme 1). The formation of ethers **3a**–**g** seems to be significant for two reasons: firstly, it is likely that, as mentioned above, to possess antiviral activity the hydroxy group should be alkylated; secondly, the Mannich bases result stabilized in acidic media and thus soluble hydrochlorides could be easily produced. To generate the alkyl

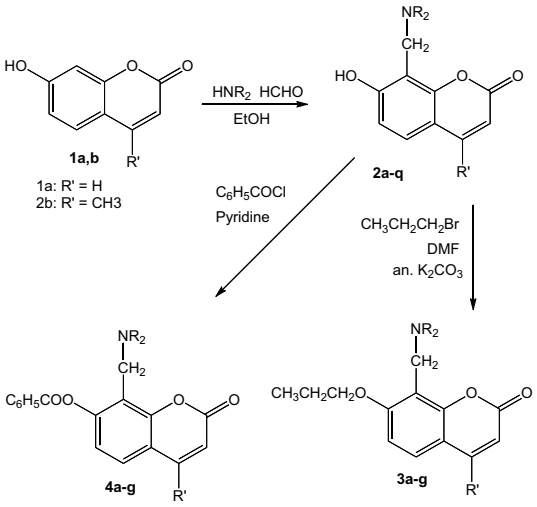

Compound	NR_2	R'
2a		H
2b, 3a		CH_3
2c		H
2d, 3b, 4a		CH_3
2e		H
2f, 4b		CH_3
2g	$N(CH_3)CH_2COOH$	H
2h	$N(CH_3)CH_2COOH$	CH_3
2i, 3c, 4c		H
2j, 3d, 4d		CH_3
2k, 3e		H
2l, 3f, 4e		CH_3
2m, 4f		H
2n		CH_3
2o		H
2p, 3g		CH_3
2q, 4g		CH_3

Scheme 1.

derivatives, we utilized *n*-propyl bromide in *N*,*N*-dimethylformamide, in the presence of anhydrous potassium carbonate, since alkylation with methyl iodide, dimethylsulfate, and diethylsulfate also yielded the quaternary ammonium salts. On the other hand, obtaining the ether derivatives before performing the Mannich reaction has no use for our purposes since, to insert the dialkylaminomethyl group in position 8, the hydro-

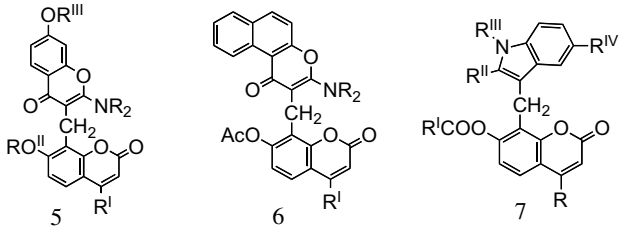

Figure 1. Unsymmetrical methylene derivatives.

xy group must be free to activate that position. So, as a first approach in this pharmacological survey, the constrained choice of propylation seems to be a reasonable compromise in collecting useful data, leaving more in-depth examination of other ether derivatives for the future.

The same philosophy was followed in the acylation reaction. It is interesting to note that it is not possible to obtain the acyl derivatives on the hydroxy group in position 7 simply by using anhydrides. In fact, the treatment of such Mannich bases with acetic or propionic anhydride leads to methylene-bis-derivatives as already described.[24,25] The formation of ester derivatives **4a**–**g** was easily accomplished by treatment of **2** with benzoyl chloride in pyridine (Scheme 1). In this case too, other investigations can be the subject of future research.

The treatment of the Mannich bases of the 7-hydroxycoumarin with acetic or propionic anhydride in the presence of compounds possessing a suitable nucleophilic center, as position 3 of 2-(dialkylamino)chromones or position 3 of indoles, leads to unsymmetrical methylene derivatives **5**–**7** (Fig. 1). The mechanism of this reaction has already been reported.[25] Moreover, to verify the general application of anhydrides in this reaction, the glutaric anhydride was also used. In this case, compounds **7g** [R = H, $R^{I} = (CH_2)_3COOH$, $R^{II} = CH_3$, $R^{III} = R^{IV} = H$] and **7h** [R = CH_3, $R^{I} = (CH_2)_3COOH$, $R^{II} = CH_3$, $R^{III} = R^{IV} = H$], bearing a carboxylic group in the side chain, were easily obtained.

All synthesized compounds are white crystals and their structures are in agreement with elemental analyses and spectral data.

Table 1. Antiviral activity of compounds **2a**–**q**, **3a**–**g**, **4a**–**g** against the RNA viruses indicated and their cytotoxicity against MT-4 cells

Compound	MT-4[a]	BVDV[b]	YFV[c]	RSV[d]
2a	>100	>100	>100	>100
2b	>100	>100	>100	>100
2c	>100	>100	>100	>100
2d	>100	>100	>100	>100
2e	>100	>100	>100	>100
2f	>100	>100	>100	>100
2g	>100	>100	>100	>100
2h	>100	>100	>100	>100
2i	>100	>100	>100	>100
2j	>100	>100	>100	>100
2k	5	>24	>59	>100
2l	28	>18	>53	>100
2m	13	>100	>100	>100
2n	72	75	>100	>100
2o	18	>100	>100	>100
2p	59	>100	>100	>100
2q	>100	>100	>100	⩾100
3a	>100	38	>100	>100
3b	>100	>100	>100	>100
3c	11	>11	>19	>25
3d	>100	20	>100	>93
3e	16	15	>48	>100
3f	>100	27	>53	>100
3g	25	8	>100	>100
4a	>100	>100	>100	>100
4b	>100	>100	>100	>100
4c	>100	>100	>100	1
4d	>100	>100	>100	18
4e	45	19	>100	>80
4f	74	77	>100	85
4g	>100	>100	>100	90
NM108[e]	>100	4	1	>100
NM 299[e]	0.2	>25	25	1

[a] Compd concn (μM) required to reduce the viability of mock-infected MT-4 (CD4+ Human T-cells containing an integrated HTLV-1 genome) cells by 50%, as determined by the colorimetric MTT method.

[b] Compd concn (μM) required to achieve 50% protection of MDBK cells from the BVDV (bovine viral diarrhea virus)-induced cytopathogenicity, as determined by the MTT method.

[c] Compd concn (μM) required to achieve 50% protection of BHK (kidney fibroblast) cells from the YFV (yellow fever virus)-induced cytopathogenicity, as determined by the MTT method.

[d] Compd concn (μM) required to reduce the plaque number of RSV (respiratory syncytial virus) by 50% in VERO-76 monolayers.

[e] Reference compounds: NM108 2′-C-Me-guanosine NM299 6-Aza-Uridine.

3. Results

3.1. Pharmacology

In the following tables the activity of compounds **2**–**4** (Table 1), **5** (Table 2), **6** (Table 3) and **7** (Table 4) against Flaviviridae and RSV is shown. All compounds were also tested against CVB-2, Sb-1, VSV, VV, Reo and HIV-1. Against this panel of viruses all the compounds resulted totally inactive (data not shown).

3.2. Molecular modeling

Since compounds **3** showed encouraging activity against BVDV, they were submitted to a molecular modeling study 'in silico' to evaluate the efficacy of such compounds to bind the surface of the most relevant HCV enzymes.

In general, all compounds **3** presented similar behavior in this molecular modeling study: indeed, such molecules resulted well fitted only on the surface of NS5B of HCV. With regards to this, for better clarity, we will give some details of compound **3d**, as an example.

Figure 2 shows the optimized location of compound **3d** within the surface binding site of HCV RdRp. The inhibitor is well buried within the lining cleft. The *n*-propyl-ether group is deeply inserted into the cavity, thus maximizing its interactions with the side chain of Arg

Table 2. Antiviral activity of compounds **5a**–**k** against the RNA viruses indicated and their cytotoxicity against MT-4 cells

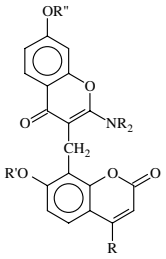

5

Compound	NR_2	R	R′	R″	MT-4[a]	BVDV[b]	YFV[c]	RSV[d]
5a	$N(CH_3)_2$	H	CH_3CO	CH_3	26	>51	>100	>25
5b	$N(CH_3)_2$	CH_3	CH_3CO	CH_3	42	>28	>100	25
5c	$N(C_2H_5)_2$	H	CH_3CO	CH_3	83	>100	>100	20
5d	$N(C_2H_5)_2$	CH_3	H	CH_3	>100	>100	>100	>100
5e	$N(C_2H_5)_2$	CH_3	CH_3CO	CH_3CO	44	>100	>100	11
5f	$N(C_2H_5)_2$	CH_3	CH_3CO	$CH_3(CH_2)_7$	>100	>100	>100	>100
5g	Pirrolidin-1-yl	H	H	CH_3	>100	>100	>100	>100
5h	Pirrolidin-1-yl	CH_3	H	CH_3	>100	>100	>100	>100
5i	Piperidin-1-yl	H	CH_3CO	CH_3	>100	>100	>100	>100
5j	$N(CH_2CH_2OCH_3)_2$	H	CH_3CO	CH_3	>100	>100	>100	7
5k	$N(CH_2CH_2OCH_3)_2$	CH_3	CH_3CO	CH_3	>100	61	>100	5
NM108[e]					>100	4	1	>100
NM 299[e]					0.2	>25	25	1

[a] Compd concn (μM) required to reduce the viability of mock-infected MT-4 (CD4+ Human T-cells containing an integrated HTLV-1 genome) cells by 50%, as determined by the colorimetric MTT method.
[b] Compd concn (μM) required to achieve 50% protection of MDBK cells from the BVDV (bovine viral diarrhea virus)-induced cytopathogenicity, as determined by the MTT method.
[c] Compd concn (μM) required to achieve 50% protection of BHK (kidney fibroblast) cells from the YFV (yellow fever virus)-induced cytopathogenicity, as determined by the MTT method.
[d] Compd concn (μM) required to reduce the plaque number of RSV (respiratory syncytial virus) by 50% in VERO-76 monolayers.
[e] Reference compounds: NM108 2′-C-Me-guanosine NM299 6-Aza-Uridine.

Table 3. Antiviral activity of compounds **6a**–**f** against the RNA viruses indicated and their cytotoxicity against MT-4 cells

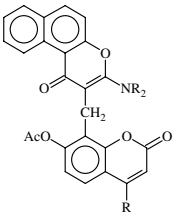

6

Compound	NR_2	R	MT-4[a]	BVDV[b]	YFV[c]	RSV[d]
6a	$N(CH_3)_2$	H	80	>48	>52	>30
6b	$N(C_2H_5)_2$	H	>100	>100	>100	>100
6c	$N(C_2H_5)_2$	CH_3	>100	>100	>100	13
6d	Piperidin-1-yl	H	>100	59	77	40
6e	$N(CH_2CH_2OCH_3)_2$	H	>100	78	100	5
6f	$N(CH_2CH_2OCH_3)_2$	CH_3	>100	>100	>100	$\geqslant$100
NM108[e]			>100	4	1	>100
NM 299[e]			0.2	>25	25	1

[a] Compd concn (μM) required to reduce the viability of mock-infected MT-4 (CD4+ Human T-cells containing an integrated HTLV-1 genome) cells by 50%, as determined by the colorimetric MTT method.
[b] Compd concn (μM) required to achieve 50% protection of MDBK cells from the BVDV (bovine viral diarrhea virus)-induced cytopathogenicity, as determined by the MTT method.
[c] Compd concn (μM) required to achieve 50% protection of BHK (kidney fibroblast) cells from the YFV (yellow fever virus)-induced cytopathogenicity, as determined by the MTT method.
[d] Compd concn (μM) required to reduce the plaque number of RSV (respiratory syncytial virus) by 50% in VERO-76 monolayers.
[e] Reference compounds: NM108 2′-C-Me-guanosine NM299 6-Aza-Uridine.

Table 4. Antiviral activity of compounds **7a**–**q** against the RNA viruses indicated and their cytotoxicity against MT-4 cells

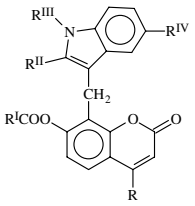

7

Compound	R	R^I	R^{II}	R^{III}	R^{IV}	MT-4[a]	BVDV[b]	YFV[c]	RSV[d]
7a	H	CH_3CH_2	H	H	H	65	⩾55	>52	>54
7b	CH_3	CH_3	H	H	OCH_3	72	>100	>100	>100
7c	H	CH_3	CH_3	H	H	62	>86	>73	>100
7d	CH_3	CH_3	CH_3	H	H	41	>100	>100	25
7e	H	CH_3CH_2	CH_3	H	H	80	>51	>100	>100
7f	CH_3	CH_3CH_2	CH_3	H	H	31	>87	>100	45
7g	H	$HOOC(CH_2)_3$	CH_3	H	H	27	>67	>100	>92
7h	CH_3	$HOOC(CH_2)_3$	CH_3	H	H	29	>69	>64	>100
7i	H	CH_3	C_6H_5	H	H	>100	>57	>100	>100
7j	CH_3	CH_3	C_6H_5	H	H	>100	>100	>100	>100
7k	H	CH_3CH_2	C_6H_5	H	H	>100	>100	>82	>100
7l	CH_3	CH_3CH_2	C_6H_5	H	H	38	7	>27	>100
7m	H	CH_3	$OCOC_2H_5$	H	H	67	>64	>72	60
7n	CH_3	CH_3	H	H	H	100	⩾100	>81	>100
7o	CH_3	CH_3	CH_3	CH_3	H	24	>40	>58	26
NM108[e]						>100	4	1	>100
NM 299[e]						0.2	>25	25	1

[a] Compd concn (μM) required to reduce the viability of mock-infected MT-4 (CD4+ Human T-cells containing an integrated HTLV-1 genome) cells by 50%, as determined by the colorimetric MTT method.

[b] Compd concn (μM) required to achieve 50% protection of MDBK cells from the BVDV (bovine viral diarrhea virus)-induced cytopathogenicity, as determined by the MTT method.

[c] Compd concn (μM) required to achieve 50% protection of BHK (Kidney fibroblast) cells from the YFV (yellow fever virus)-induced cytopathogenicity, as determined by the MTT method.

[d] Compd concn (μM) required to reduce the plaque number of RSV (respiratory syncytial virus) by 50% in VERO-76 monolayers.

[e] Reference compounds: NM108 2′-C-Me-guanosine NM299 6-Aza-Uridine.

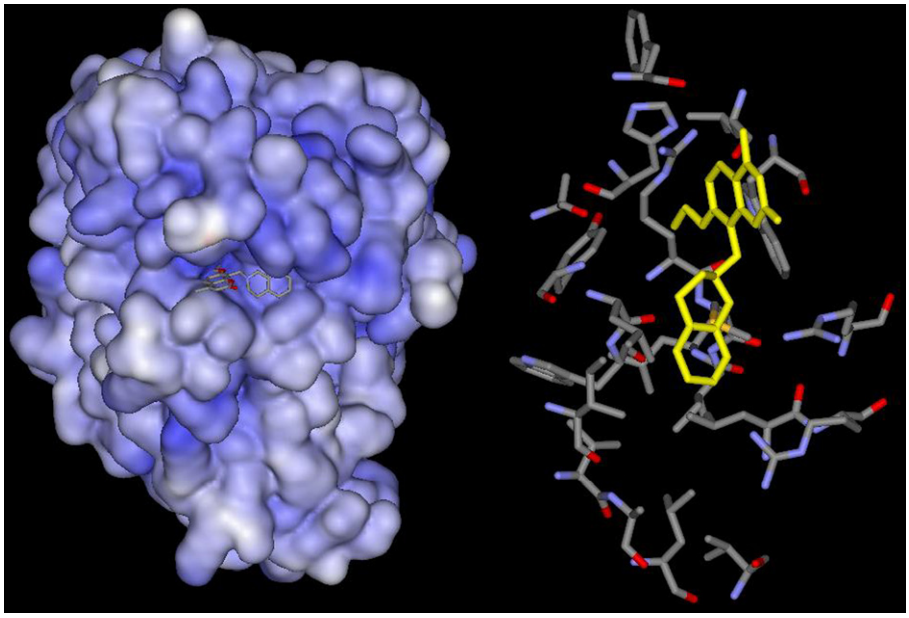

Figure 2. Optimized binding mode for compound **3d** into the allosteric binding site of NS5B of HCV (left). Details of the binding site (right). In this figure, hydrogen atoms and water molecules are omitted for clarity.

422, His 475, Tyr 477, and Trp 528. The tetrahydroisoquinoline moiety is surrounded by a series of apolar main and side chain atoms of Leu 419, Met 423, Ile 482, and Arg 501.

Table 5. Energy terms and total free energy of binding (kcal/mol) between HCV RdRp and compounds **3a**–**g**

	3a	**3b**	**3c**	**3d**	**3e**	**3f**	**3g**
ΔE_{VDW}	−44.66	−45.29	−47.90	−45.88	−44.77	−44.82	−46.65
ΔE_{EL}	−14.83	−12.67	−12.55	−11.21	−15.54	−13.74	−14.33
ΔE_{MM}	−59.49	−57.96	−60.45	−57.09	−60.31	−58.56	−60.98
ΔG_{PB}	42.42	46.78	47.29	44.91	46.07	42.89	45.57
ΔG_{NP}	−4.21	−5.05	−4.53	−4.85	−4.96	−4.09	−4.99
$-T\Delta S$	15.05	10.70	11.11	10.88	12.76	13.79	12.63
ΔG_{bind}	−6.23	−5.53	−6.58	−6.15	−6.44	−5.97	−7.77
Calc. IC_{50}	27	88	15	31	19	42	2
Exp. EC_{50}	38	>100	>11	20	15	27	8

Calculated IC_{50} and experimental EC_{50} values are in μM.

Furthermore, the analysis of the dynamic trajectory reveals a partial π–π stacking between this group and the phenyl moiety of Tyr 477.

Further insights into the forces involved in substrate binding can be obtained by analyzing the free energy of binding and its components, which are listed in Table 5 for all type **3** compounds.

4. Discussion

It is possible to draw the following considerations from the above results.

The Mannich bases derived from 7-hydroxycoumarins, namely compounds **2**, are generally inactive regarding the tested viruses. In particular, cinnamyl derivatives **2k** and **2l** as well as benzodioxol derivative **2m** and acetylphenyl derivative **2o** are cytotoxic.

The series of propyloxy derivatives **3** appears, on the whole, to be endowed with some activity against BVDV, whereas they are inactive against YFV and RSV. In particular, the tetrahydroisoquinoline derivative **3d**, the cinnamyl derivative **3e**, and the acetylphenyl derivative **3g** resulted active against BVDV, but compounds **3e** and **3g** showed a certain degree of toxicity. It is interesting to note that, in this series, the presence of the methyl substituent in position 4 does seem to favor antiviral activity. In this regard, it is valuable to remember that position 4 of Osthole does not support any substituent.

The benzoyl derivatives **4** seem, generally, inactive or moderately active against BVDV. It is important to note the remarkable action of tetrahydroisoquinoline derivatives **4c** and **4d** against RSV without sign of toxicity. In particular, compound **4c** shows a high level of activity and this type of action needs to be validated by further data.

Benzopyran and naphthopyran derivatives **5** and **6** do not show appreciable activity against BVDV and YFV. It is possible to note some level of activity against RSV.

The series of indole derivatives **7** shows, on the whole, remarkable toxicity; **7l** being the most active compound against BVDV.

In conclusion, the most interesting compounds against HCV-related viruses appear to be the propyloxy derivatives **3**. In this regard, it is possible to draw a correspondence with Osthole in which the presence of a 7-methoxy group is mandatory.

Benzoyl compounds **4** present a moderate interest against HCV-related virus. Also compounds with a methylene bridge **5**–**7** do not have a significant interest against HCV-related viruses, with the only exception of **7l**. Occasionally, activity may emerge against other viruses (in particular RSV). Some of these (**4c**, **5j**, **5k**, **6e**) deserve deeper insight.

Since derivatives **3** are, in general, endowed with remarkable activity against BVDV, we were interested in testing their possible action on HCV studying the docking of our molecules into the pocket of RNA-dependent RNA polymerase (RdRp) of HCV by computer assisted methods.

As we may see from Table 5, both the intermolecular van der Waals and the electrostatics are important contributions to the binding. However, comparing the van der Waals/non-polar ($\Delta E_{VDW} + \Delta G_{NP}$) with the electrostatic ($\Delta E_{EL} + \Delta G_{PB}$) contributions for all molecules, we can see that in all cases the association between inhibitors and the target protein is mainly driven by more favorable non-polar interactions in the complex rather than in solution. When examining the role of the electrostatics in the inhibitor–enzyme complex formation, it is however fundamental to consider the electrostatic component of the molecular mechanical energy ΔE_{EL} together with the electrostatic contribution to solvation, ΔG_{PB}. Indeed, electrostatics generally disfavor the docking of ligand and receptor molecules. The unfavorable change in the electrostatics of solvation is mostly, but not fully, compensated by the favorable electrostatics within the resulting ligand–receptor complex. Indeed, the total electrostatic energy contributions for all protein/drug complex formations are all unfavorable; the **3a**, **3e**, and **3g**/protein complex formations being less unfavorable than the remaining compound complex formations because of a less positive total electrostatic term, in which the penalty paid by the electrostatics of solvation is better compensated by favorable electrostatic interactions within the complex. Thus, even though electrostatics destabilize inhibitor/protein complex formation, it is the optimized balance of opposing

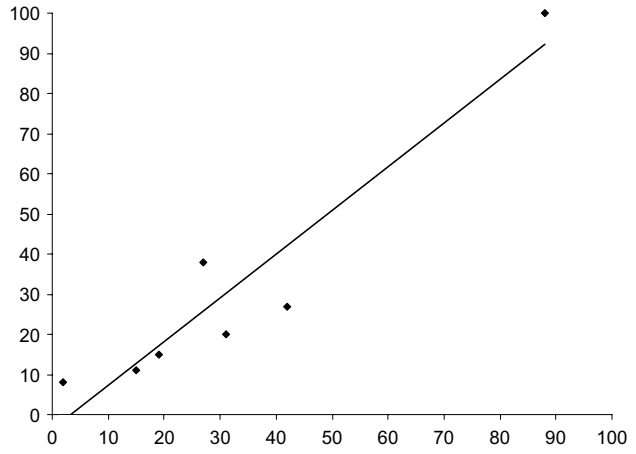

Figure 3. Correlation between calculated IC_{50} (*x*-axis) and experimental EC_{50} (*y*-axis). Values are in μM. Trendline with $R^2 = 0.896$.

electrostatic contributions that leads to tighter binding in the series of compounds **3a**, **3c**, **3e**, and **3g**.

Interestingly, the values of IC_{50}, reported in Table 5 and calculated on the basis of Eq. 6 (see Experimental) for binding to HCV RdRp, compare well with the corresponding experimental data, expressed in terms of EC_{50} on cells infected with BVDV. In Figure 3 we report a correlation graph between calculated IC_{50} and experimental IC_{50} with trendline calculated ($R^2 = 0.896$). This can be taken both as a clue that the RdRp is the effective protein target for these compounds, and as a positive indication of activity of these molecules against HCV.

Molecular dynamics simulations have shown to be able to rank binding affinities of the most active molecules, to provide insight into the interactions occurring in the active site of the most probable target (the HCV RdPp), and to rationalize the origins of variations in the corresponding binding free energy. Accordingly, the computational strategy used in this paper can provide a blueprint for new inhibitors in structure-based drug design or in predicting binding affinity of a ligand prior to organic synthesis.

5. Conclusions

In the present study, we have synthesized some Mannich bases of 7-hydroxycoumarins (**2**) and related compounds (**3**–**7**) in order to investigate their ability in counteracting the replication of Flaviviridae.

Our results indicate that the Mannich bases of 7-hydroxycoumarins (**2**), having a free hydroxy group in position 7, do not convey any antiviral activity. On the other hand, the formation of ethers in that position (compounds **3**) leads to derivatives endowed with remarkable antiviral activity on HCV-related viruses. Interestingly, the above-mentioned behavior of the hydroxy/alkoxy groups in position 7 is analogous to that of Osthenol/Osthole, which present some structural similarity to our compounds.

The corresponding esters (compounds **4**) have poor efficacy against HCV-related viruses, but some of them deserve deeper insight for their activity against RSV. Unsymmetrical methylene derivatives (compounds **5**–**7**) are, generally, lacking in activity on HCV-related viruses but present a certain interest against RSV.

Since propyloxy derivatives **3** could be a candidate as a lead structure for drugs against HCV, the use of molecular modeling indicates that an allosteric receptor of NS5B protein of HCV could be involved in the activity of our compounds. The good correlation between found and calculated IC_{50}, as depicted in Table 5, corroborates that proposal.

Finally, this study has highlighted a new type of activity of the 7-hydroxycoumarin derivatives and, following this promising route, many other Mannich bases of 7-hydroxycoumarin are under investigation in the search for antiviral drugs. The second part of this study will be devoted to the synthesis of Mannich bases between 7-hydroxycoumarins and secondary diamines.

6. Experimental

6.1. General

Melting points were determined using an Electrothermal apparatus and are uncorrected. Microanalyses were carried out on a Carlo Erba 1106 elemental analyzer. ^{1}H NMR and ^{13}C NMR spectra were performed on a Varian Gemini 200 (200 MHz) spectrometer using TMS as internal standard ($\delta = 0$). IR spectra were recorded on a Perkin-Elmer 398 Spectrophotometer. The synthesis of compounds **5**–**7** are reported in Refs. 23–25.

6.2. Mannich bases 2

6.2.1. General method. To 20.0 mmol of 7-hydroxycoumarin (or 4-methyl-7-hydroxycoumarin) dissolved in 20 ml of 95% ethanol, 20.0 mmol of the appropriate amine (A) and 2.0 ml of 40% formaldehyde were added. The resulting mixture was refluxed for 4–6 h. After cooling, the solvent was evaporated under reduced pressure. The pale yellow oil obtained was treated with a little amount of cool acetone, leaving a white solid crystallized from suitable solvent (B) obtaining:

6.2.1.1. 8-Piperidinomethyl-7-hydroxycoumarin (2a). (A) piperidine; (B) acetone. The compound is already described.[25]

6.2.1.2. 8-Piperidinomethyl-4-methyl-7-hydroxycoumarin (2b). (A) piperidine; (B) acetone. The compound is already described.[25]

6.2.1.3. 8-Morpholinomethyl-7-hydroxycoumarin (2c). (A) morpholine; (B) acetone. The compound is already described.[37]

6.2.1.4. 7-Hydroxy-4-methyl-8-morpholinomethylcoumarin (2d). (A) morpholine; (B) acetone. The compound is already described.[37]

6.2.1.5. 7-Hydroxy-8-[(4-methyl)piperazin-1-yl]methylcoumarin (2e). (A) *N*-methylpiperazine; (B) acetone. Mp 168–169 °C; yield 57%. IR (KBr), ν(cm^{-1}): 3416 (broad), 2950, 2831, 1714, 1607, 1238. ^{1}H NMR ($CDCl_3$), δ: 3.22 (s, 3H, –N–CH_3), 4.00–4.37 (m, 8H, –N–CH_2), 4.99 (s, 2H, CH_2 bridge), 6.68 (d, J = 9, 1H, H-3), 7.26 (d, J = 10, 1H, H-6), 7.83 (d, J = 10, 1H, H-5), 8.13 (d, J = 9, 1H, H-4). ^{13}C NMR ($CDCl_3$), δ: 45.0 (N–CH_3), 51.7 (α N–CH_2), 52.7 (CH_2 bridge), 53.9 (β N–CH_2), 106.7 (C-6), 110.5 (C-9), 110.7 (C-3), 113.0 (C-8), 127.3 (C-5), 143.5 (C-4), 152.3 (C-10), 160.4 (C-7), 161.9 (C-2). Anal. Calcd for $C_{15}H_{18}N_2O_3$: C, 65.68; H, 6.61; N 10.21. Found: C, 65.79; H, 6.59; N, 10.15.

6.2.1.6. 7-Hydroxy-4-methyl-8-[(4-methyl)piperazin-1-yl]methylcoumarin (2f). (A) *N*-methylpiperazine; (B) acetone. Mp 132–134 °C; yield 55%. IR (KBr), ν(cm^{-1}): 3502 (broad), 2953, 2823, 1727, 1279. ^{1}H NMR (CF_3COOD), δ: 2.65 (s, 3H, 4-CH_3), 3.25 (s, 3H, –N–CH_3), 4.00–4.37 (m, 8H, –N–CH_2), 4.99 (s, 2H, CH_2 bridge), 6.68 (s, 1H, H-3), 7.30 (d, J = 9, 1H, H-6), 8.02 (d, J = 9, 1H, H-5). Anal. Calcd for $C_{16}H_{20}N_2O_3$: C, 66.65; H, 6.99; N, 9.72. Found: C, 66.87; H, 7.08; N, 9.68.

6.2.1.7. 7-Hydroxy-8-(sarcosin-*N*-yl)methylcoumarin (2g). (A) sarcosine; (B) ethanol. Mp 209–211 °C; yield 56%. IR (KBr), ν(cm^{-1}): 3411, 2958, 2823, 1717, 1630, 1247. ^{1}H NMR (CF_3COOD), δ: 3.30 (s, 3H, N–CH_3), 4.41 (s, 2H, N–CH_2–COOH), 5.02 (s, 2H, CH_2 bridge), 6.63 (d, J = 10, 1H, H-3), 7.25 (d, J = 9, 1H, H-6), 7.85 (d, J = 9, 1H, H-5), 8.13 (d, J = 10, 1H, H-4). Anal. Calcd for $C_{13}H_{13}NO_5$: C, 59.31; H, 4.98; N, 5.32. Found: C, 59.06; H, 5.05; N, 5.28.

6.2.1.8. 7-Hydroxy-4-methyl-8-(sarcosin-*N*-yl)methylcoumarin (2h). (A) sarcosine; (B) acetone. Mp 219–221 °C; yield 58%. IR (KBr), ν(cm^{-1}): 3407, 2964, 2822, 1725, 1631, 1225. ^{1}H NMR (CF_3COOD), δ: 2.65 (s, 3H, 4-CH_3), 3.35 (s, 3H, N–CH_3), 4.41 (s, 2H, N–CH_2–COOH), 5.02 (s, 2H, CH_2 bridge), 6.65 (s, 1H, H-3), 7.30 (d, J = 10, 1H, H-6), 8.02 (d, J = 10, 1H, H-5). Anal. Calcd for $C_{14}H_{15}NO_5$: C, 60.64; H, 5.45; N, 5.05. Found: C, 60.79; H, 5.37; N, 5.14.

6.2.1.9. 7-Hydroxy-8-(tetrahydroisoquinolin-1-yl)methylcoumarin (2i). (A) tetrahydroisoquinoline; (B) acetone. Mp 182–184 °C; yield 65%. IR (KBr), ν(cm^{-1}): 3024, 2917, 2834, 1713, 1606, 1238. ^{1}H NMR ($CDCl_3$), δ: 2.90–3.20 (m, 4H, α + β –N–CH_2–CH_2-Ar tetrahydroisoquinoline), 3.85 (s, 2H, N–CH_2–Ar), 4.25 (s, 2H, CH_2 bridge), 6.25 (d, J = 9, 1H, H-3), 6.80 (d, J = 7, 1H, H-6), 7.05–7.50 (m, 5H, H-5, H arom. tetrahydroisoquinoline), 7.70 (d, J = 9, 1H, H-4). ^{13}C NMR ($CDCl_3$), δ: 27.7 (C-7′), 49.4 (C-2′), 52.5 (CH_2 bridge), 54.5 (C-8′), 106.9 (C-6), 110.6 (C-9), 110.8 (C-3), 113.2 (C-8), 125.4 (C-4′), 125.9 (C-5′), 126.1 (C-6′), 127.5 (C-5), 128.0 (C-3′), 131.9 (C-9′), 132.3 (C-10′), 143.6 (C-4), 152.5 (C-10), 160.6 (C-7), 162.1 (C-2). Anal. Calcd for $C_{19}H_{17}NO_3$: C, 74.25; H, 5.58; N, 4.56. Found: C, 74.48; H, 5.65; N, 4.50.

6.2.1.10. 7-Hydroxy-4-methyl-8-(tetrahydroisoquinolin-1-yl)methylcoumarin (2j). (A) tetrahydroisoquinoline; (B) ethanol. Mp 166–168 °C; yield 67%. IR (KBr), ν(cm^{-1}): 2952, 2839, 1702, 1603, 1290. ^{1}H NMR ($CDCl_3$), δ: 2.40 (s, 3H, 4-CH_3), 2.85–3.10 (m, 4H, α β –N–CH_2–CH_2–Ar tetrahydroisoquinoline), 3.85 (s, 2H, –N–CH_2–Ar), 4.25 (s, 2H, CH_2 bridge), 6.15 (s, 1H, H-3), 6.80 (d, J = 9, 1H, H-6), 7.05–7.35 (m, 4H, H arom. tetrahydroisoquinoline), 7.50 (d, J = 9, 1H, H-5), 10.49 (br s, 1H, OH). Anal. Calcd for $C_{20}H_{19}NO_3$: C, 74.75; H, 5.96; N, 4.36. Found: C, 74.84; H, 6.06; N, 4.37.

6.2.1.11. 8-(*trans*-4-Cinnamylpiperazin-1-yl)methyl-7-hydroxycoumarin (2k). (A) *trans*-1-cinnamylpiperazine; (B) ethanol. Mp 128–130 °C; yield 62%. IR (KBr), ν(cm^{-1}): 3412 (broad), 2938, 2825, 1713, 1606, 1233. ^{1}H NMR ($CDCl_3$), δ: 2.56–2.86 (m, 8H, –N–CH_2), 3.22 (d, 2H, –N–*CH_2*–CH═), 4.09 (s, 2H, CH_2 bridge), 6.22 (d, J = 8, 1H, H-3), 6.35–6.54 (m, 2H, Ar–CH═CH–), 6.66–7.79 (m, 8H, H-4, H-5, H-6, H arom.). Anal. Calcd for $C_{23}H_{24}N_2O_3$: C, 73.38; H, 6.43; N, 7.44. Found: C, 73.23; H, 6.46; N, 7.38.

6.2.1.12. 8-(*trans*-4-Cinnamylpiperazin-1-yl)methyl-7-hydroxy-4-methylcoumarin (2l). (A) *trans*-4-cinnamylpiperazine; (B) ethyl acetate. Mp 156–158 °C; yield 63%. IR (KBr), ν(cm^{-1}): 2938, 2807, 1721, 1601, 1285. ^{1}H NMR($CDCl_3$), δ: 2.34 (s, 3H, 4-CH_3), 2.51–2.86 (m, 8H, N–CH_2), 3.18 (d, J = 6, 2H, –N–*CH_2*–CH═), 4.07 (s, 2H, CH_2 bridge), 6.08 (s, 1H, H-3), 6.30–6.51 (m, 2H, Ar–CH═CH–), 6.65–7.55 (m, 7H, H-5, H-6, H arom.), 10.17 (s, 1H, OH). Anal. Calcd for $C_{24}H_{26}N_2O_3$: C, 73.82; H, 6.71; N 7.17. Found: C, 74.08; H, 6.80; N 7.08.

6.2.1.13. 8-{4-[(1,3-Benzodioxol-5-yl)methyl]piperazin-1-yl}methyl-7-hydroxycoumarin (2m). (A) 1-piperonylpiperazine; (B) ethyl acetate. Mp 182–183 °C; yield 42%. IR (KBr), ν(cm^{-1}): 3060, 2958, 2837, 1737, 1598, 1244. ^{1}H NMR ($CDCl_3$+DMSO-d_6), δ: 2.68–2.90 (m, 4H, β N–CH_2), 3.25–3.70 (m, 4H, α N–CH_2), 3.91 (s, 2H, N–CH_2–Ar), 3.98 (s, 2H, CH_2 bridge), 6.06 (s, 2H, O–CH_2O), 6.46 (d, J = 10, 1H, H-3), 6.75–8.32 (m, 6H, H-4, H-5, H-6, H arom.), 10.21 (br s, 1H, OH). Anal. Calcd for $C_{22}H_{22}N_2O_5$: C, 66.99; H, 5.62; N, 7.10. Found: C, 67.14; H, 5.55; N, 7.05.

6.2.1.14. 8-{4-[(1,3-Benzodioxol-5-yl)methyl]piperazin-1-yl}methyl-7-hydroxy-4-methylcoumarin (2n). (A) 1-piperonylpiperazine; (B) ethyl acetate. Mp 151–152 °C; yield 47%. IR (KBr), ν(cm^{-1}): 3413, 2949, 2811, 1719, 1605, 1235. ^{1}H NMR($CDCl_3$), δ: 2.42 (s, 3H, 4-CH_3), 2.52–2.90 (m, 4H, β N–CH_2), 3.45–3.60 (m, 4H, α N–CH_2), 4.08–4.25 (m, 4H, –N–CH_2–Ar, CH_2 bridge), 6.02 (s, 2H, O–CH_2O), 6.18–7.65 (m, 5H, H-5, H-6, H arom.). Anal. Calcd for $C_{23}H_{24}N_2O_5$: C, 67.63; H, 5.92; N 6.86. Found: C, 67.53; H, 5.99; N 6.78.

6.2.1.15. 8-[4-(4-Acetlyphen-1-yl)piperazin-1-yl]methyl-7-hydroxycoumarin (2o). (A) 4′-piperazinoacetophenone; (B) ethyl acetate. Mp 162–164 °C; yield 65%. IR (KBr), ν(cm^{-1}): 3444, 2947, 2818, 1717, 1664, 1601, 1235. ^{1}H NMR ($CDCl_3$), δ: 2.46 (s, 3H, CH_3–CO), 2.65–2.92 (m, 4H, β N–CH_2), 3.25–3.50 (m, 4H, α N–CH_2), 4.06 (s, 2H, CH_2 bridge), 6.14 (d, J = 9.4, 1H, H-3), 6.72 (d, J = 8.6, 1H, H-6), 6.82 (d, J = 7.6, 2H, β arom.), 7.24 (d, J = 8,6, 1H, H-5), 7.57 (d, J = 9.4, 1H, H-4), 7.82 (d, J = 7.6, 2H, α arom.). ^{13}C NMR ($CDCl_3$), δ: 25.4 (CH_3), 46.5 (β N–CH_2), 51.5 (α N–CH_2), 52.7 (CH_2 bridge), 106.5 (C-6), 110.8 (C-9), 111.0 (C-3), 113.1 (C-8, C-2′,6′), 127.6 (C-5, C-4′), 129.6 (C-3′,5′), 143.5 (C-4), 152.4 (C-10), 152.9 (C-1′), 160.4 (C-7), 161.5 (C-2), 195.8 (CO). Anal. Calcd for $C_{22}H_{22}N_2O_4$: C, 69.83; H, 5.86; N 7.40. Found: C, 70.05; H, 5.88; N 7.49.

6.2.1.16. 8-[4-(4-Acetlyphen-1-yl)piperazin-1-yl]methyl-7-hydroxy-4-methylcoumarin (2p). (A) 4′-piperazinoacetophenone; (B) ethyl acetate. Mp 217–218 °C; yield 63%. IR (KBr), ν(cm^{-1}): 3413, 2947, 2843, 1716, 1702, 1662, 1596, 1237. ^{1}H NMR ($CDCl_3$), δ: 2.39 (s, 3H, CH_3–CO), 2.51 (s, 3H, 4-CH_3), 2.68–2.93 (m, 4H, β N–CH_2), 3.31–3.55 (m, 4H, α N–CH_2), 4.14 (s, 2H, CH_2 bridge), 6.12 (s, 1H, H-3), 6.78 (d, J = 8.4, 1H, H-6), 6.92 (d, J = 7.6, 2H, β arom.), 7.42 (d, J = 8.4, 1H, H-5), 7.94 (d, J = 7.6, 2H, α arom.). Anal. Calcd for $C_{23}H_{24}N_2O_4$: C, 70.39; H, 6.16; N, 7.14. Found: C, 70.49; H, 6.11; N, 7.05.

6.2.1.17. 8-[4-(Ethoxycarbonyl)piperazin-1-yl]methyl-7-hydroxy-4-methylcoumarin (2q). (A) ethyl 1-piperazinecarboxylate; (B) ethyl acetate. Mp 137–138 °C; yield 48%. IR (KBr), ν(cm^{-1}): 3440, 2950, 2867, 1731, 1709, 1603, 1287. ^{1}H NMR ($CDCl_3$), δ: 1,26 (t, J = 6, 3H, CH_3–CH_2), 2.39 (s, 3H, 4-CH_3), 2.49–2.78 (m, 4H, β N–CH_2), 3.42–3.78 (m, 4H, α N–CH_2), 4.10 (s, 2H, CH_2 bridge), 4.18 (q, J = 6, 2H, CH_3–CH_2), 6.11 (s, 1H, H-3), 6.79 (d, J = 8, 1H, H-6), 7.47 (d, J = 8, 1H, H-5), 9.20 (s, 1H, OH). Anal. Calcd for $C_{18}H_{22}N_2O_5$: C, 62.42; H, 6.40; N, 8.09. Found: C, 62.19; H, 6.39; N, 8.16.

6.3. Propyl derivatives 3

6.3.1. General method. In a round-bottom flask protected from moisture with a calcium chloride dryness tube, a quantity of 2.0 mmol of Mannich base **2** was heated in 10 ml of *N*,*N*-dimethylformamide until dissolution was completed, then 0.3 g of anhydrous potassium carbonate and 2.0 mmol (0.23 g) of 1-bromopropane were added. The mixture was heated at 100 °C for 5 h under a slight nitrogen stream. At the end, 15 ml of water and 20 ml of chloroform were added and the mixture was allowed to stir for 30 min. Then, the organic phase was separated out and the aqueous one was extracted again with chloroform. The pooled organic phases were dried on anhydrous sodium sulfate, filtered, and evaporated under reduced pressure. The oily residue was cooled and precipitated from ethyl ether. The precipitate was filtered and crystallized from suitable solvent. The following compounds were obtained:

6.3.1.1. 4-Methyl-8-piperidinomethyl-7-propyloxycoumarin (3a). Crystallized from ethyl acetate, mp 147–148 °C; yield 65%. IR (KBr), ν(cm^{-1}): 3425, 2933, 2850, 1720, 1605, 1569, 1292. ^{1}H NMR ($CDCl_3$+DMSO-d_6), δ: 1.10 (t, J = 5, 3H, CH_3–CH_2), 1.35–1.62 (m, 8H, CH_2 β + γ piperidine, CH_3–CH_2), 2.32–2.71 (m, 7H, $CH_2\alpha$ piperidine, 4-CH_3), 3.82 (s, 2H, CH_2 bridge), 4.08 (t, J = 5, 2H, CH_2–O), 6.15 (s, 1H, H-3), 6.94 (d, J = 9, 1H, H-6), 7.58 (d, J = 9, 1H, H-5). Anal. Calcd for $C_{19}H_{25}NO_3$: C, 72.35; H, 7.99; N, 4.44. Found: C, 72.14; H, 7.94; N, 4.52.

6.3.1.2. 4-Methyl-8-morpholinomethyl-7-propyloxycoumarin (3b). Crystallized from ethyl acetate, mp 146–147 °C; yield 52%. IR (KBr), ν(cm^{-1}): 3444, 2929, 2846, 1725, 1602, 1284. ^{1}H NMR ($CDCl_3$), δ: 1.09 (t, J = 5.5, 3H, CH_3–CH_2), 1.68–2.09 (m, 2H, CH_3–CH_2–), 2.39 (s, 3H, 4-CH_3), 2.48–2.73 (m, 4H, CH_2 α morpholine), 3.55–3.79 (m, 4H, CH_2 β morpholine), 3.89 (s, 2H, CH_2 bridge), 4.05 (t, J = 5.5, 2H, CH_2–O), 6.16 (s, 1H, H-3), 6.90 (d, J = 9.5, 1H, H-6), 7.56 (d, J = 9.5, 1H, H-5). Anal. Calcd for $C_{18}H_{23}NO_4$: C, 68.12; H, 7.30; N, 4.41. Found: C, 67.88; H, 7.40; N, 4.47.

6.3.1.3. 7-Propyloxy-8-(tetrahydroisoquinolin-1-yl)-methylcoumarin (3c). Crystallized from ethyl ether, mp 113–114 °C; yield 60%. IR (KBr), ν(cm^{-1}): 2920, 2851, 1720, 1605, 1282. ^{1}H NMR ($CDCl_3$), δ: 0.90 (m, 3H, CH_3–CH_2), 1.50–1.85 (m, 2H, CH_3–CH_2–), 2.81–3.09 (m, 4H, –N–CH_2–CH_2–Ar), 3.81 (t, 2H, CH_2–O), 3.90–4.27 (m, 4H, CH_2 bridge, –N–CH_2–Ar), 6.28 (d, J = 9, 1H, H-3), 6.78–7.82 (m, 7H, H-4, H-5, H-6, H arom.). ^{13}C NMR ($CDCl_3$), δ: 13.4 (CH_3), 25.4 (CH_3–CH_2), 31.2 (C-7′), 47.8 (C-2′), 50.3 (CH_2 bridge), 54.9 (C-8′), 68.2 (CH_2–O), 107.6 (C-6), 111.9 (C-8), 112.3 (C-3), 113.6 (C-9), 124.6 (C-4′), 125.2 (C-5′), 125.8 (C-6′), 127.3 (C-5), 127.9 (C-3′), 133.5 (C-9′), 134.4 (C-10′), 143.0 (C-4), 153.3 (C-10), 160.2 (C-7), 160.5 (C-2). Anal. Calcd for $C_{22}H_{23}NO_3$: C, 75.62; H, 6.63; N, 4.01. Found: C, 75.82; H, 6.69; N, 3.95.

6.3.1.4. 4-Methyl-7-propyloxy-8-(tetrahydroisoquinolin-1-yl)methylcoumarin (3d). Crystallized from ethyl ether, mp 114–115 °C; yield 64%. IR (KBr), ν(cm^{-1}): 2936, 2833, 1718, 1605, 1289. ^{1}H NMR ($CDCl_3$), δ: 1.16 (t, J = 5, 3H, CH_3–CH_2), 1.72–2.05 (m, 2H, –CH_2–CH_2–O–), 2.41 (s, 3H, 4-CH_3), 2.85–3.06 (m, 4H, –N–CH_2–CH_2–Ar), 3.81 (t, J = 5, 2H, –CH_2–O), 3.92–4.24 (m, 4H, CH_2 bridge, –N–CH_2–Ar tetrahydroisoquinoline), 6.20 (s, 1H, H-3), 6.90–7.69 (m, 6H, H-5, H-6, H arom.). Anal. Calcd for $C_{23}H_{25}NO_3$: C, 76.01; H, 6.93; N, 3.85. Found: C, 75.87; H, 7.01; N, 3.87.

6.3.1.5. 8-(*trans*-4-Cinnamylpiperazin-1-yl)methyl-7-propyloxycoumarin (3e). Crystallized from ethyl acetate, mp 148–149 °C; yield 54%. IR (KBr), ν(cm^{-1}): 2941, 2811, 1717, 1605, 1238. ^{1}H NMR ($CDCl_3$+DMSO-d_6), δ: 1.08 (t, J = 5, 3H, CH_3–CH_2), 1.70–2.00 (m, 2H, CH_2–CH_2–O), 2.50–2.82 (m, 8H, –N–CH_2–CH_2–N–), 3.15 (d, J = 5, 2H, –N–CH_2–CH═), 3.95 (s, 2H, CH_2 bridge), 4.05 (t, J = 5, 2H, –CH_2–O–), 6.05–7.80 (m, 10H, –CH═CH, H-4, H-5, H-6, H arom.). Anal. Calcd

for $C_{26}H_{30}N_2O_3$: C, 74.61; H, 7.22; N, 6.69. Found: C, 74.72; H, 7.12; N, 6.77.

6.3.1.6. 8-(*trans*-4-Cinnamylpiperazin-1-yl)methyl-4-methyl-7-propyloxycoumarin (3f). Crystallized from ethyl acetate, mp 123–124 °C; yield 46%. IR (KBr), ν(cm^{-1}): 2940, 2812, 1724, 1606, 1236. ^{1}H NMR ($CDCl_3$), δ: 1.06 (t, J = 5, 3H, CH_3–CH_2), 1.75–1.98 (m, 2H, CH_2–CH_2–O–), 2.38 (s, 3H, 4-CH_3), 2.45–2.80 (m, 8H, –N–CH_2–CH_2–N–), 3.11 (d, J = 5, 2H, –N–CH_2–CH═), 3.96 (s, 2H, CH_2 bridge), 4.02 (t, J = 5, 2H, –CH_2–O), 6.15 (s, 1H, H-3), 6.30–7.63 (m, 9H, –CH═CH, H-5, H-6, H arom.). Anal. Calcd for $C_{27}H_{32}N_2O_3$: C, 74.97; H, 7.46; N, 6.48. Found: C, 75.23; H, 7.55; N, 6.38.

6.3.1.7. 8-[4-(4-Acetylphen-1-yl)piperazin-1-yl]methyl-4-methyl-7-propyloxycoumarin (3g). Crystallized from ethanol, mp 147–148 °C; yield 46%. IR (KBr), ν(cm^{-1}): 2941, 2811, 1728, 1661, 1600, 1287. ^{1}H NMR ($CDCl_3$), δ: 1.02 (t, J = 6.4, 3H, CH_3–CH_2), 1.70–1.89 (m, 2H, CH_2–CH_2–O–), 2.41 (s, 3H, 4-CH_3), 2.43 (s, 3H, CH_3–CO), 2.67 (t, J = 5.2, 4H, β CH_2–N), 3.26 (t, 4H, α N–CH_2), 3.88 (s, 2H, CH_2 bridge), 3.97 (t, J = 6.4, 2H, CH_2–O), 6.18 (d, J = 9.6, 1H, H-3), 6.74 (d, J = 9.2, 2H, β arom.), 6.79 (d, J = 9.4, 1H, H-6), 7.30 (d, J = 9.6, 1H, H-4), 7.60 (d, J = 9.4 1H, H-5), 7.82 (d, J = 9.2, 2H, α arom.). ^{13}C NMR ($CDCl_3$), δ: 10.0 (CH_3–CH_2), 18.1 (4-CH_3), 21.9 (CH_3–CO), 25.4 (CH_3–CH_2), 46.5 (α N–CH_2), 47.7 (CH_2 bridge), 51.6 (β N–CH_2), 69.7 (CH_2–O), 107.6 (C-6), 111.9 (C-3), 112.3 (C-8), 112.4 (C-9), 112.5 (C-2′,6′), 126.6 (C-4′), 127.6 (C-5), 129.6 (C-3′,5′), 143.1 (C-4), 153.3 (C-1′), 153.4 (C-10), 160.2 (C-7), 160.3 (C-2), 195.7 (CO). Anal. Calcd for $C_{26}H_{30}N_2O_4$: C, 71.87; H, 6.96; N, 6.45. Found: C, 71.95; H, 6.91; N, 6.52.

6.4. Benzoyl derivatives 4

6.4.1. General method. In a round-bottom flask protected from moisture with a calcium chloride dryness tube, a quantity of 2.0 mmol of Mannich base **2** was heated in 10 ml of pyridine until dissolution was completed. Then 4.0 mmol (0.56 g) of benzoyl chloride was added. The mixture was heated at 100 °C for 3 h. At the end, after cooling, ice was added and a precipitate was formed. The solid was filtered and crystallized from ethyl ether. The following compounds were obtained:

6.4.1.1. 7-Benzoyloxy-4-methyl-8-morpholinomethylcoumarin (4a). Mp 161–162 °C; yield 50%. IR (KBr), ν(cm^{-1}): 2965, 2852, 1749, 1728, 1716, 1629, 1600, 1227. ^{1}H NMR ($CDCl_3$) δ: 2.21–2.59 (m, 7H, N–$CH_2$$CH_2$–O, 4-$CH_3$), 3.20–3.52 (m, 4H, N–$CH_2$$CH_2$–O), 3.81 (s, 2H, CH_2 bridge), 6.34 (s, 1H, H-3), 7.22 (d, J = 7, 1H, H-6), 7.45–8.43 (m, 6H, H-5+H arom.). ^{13}C NMR ($CDCl_3$), δ: 18.1 (4-CH_3), 52.0 (N–$CH_2$$CH_2$–O), 53.1 ($CH_2$ bridge), 65.7 (N–$CH_2$$CH_2$–O), 106.3 (C-6), 110.0 (C-3), 111.7 (C-9), 112.8 (C-8), 127.6 (C-3′,5′), 128.0 (C-5), 129.3 (C-2′,6′), 129.4 (C-1′), 132.6 (C-4′), 151.8 (C-10), 152.7 (C-7), 160.5 (C-4), 161.3 (C-2), 170.3 (CO). Anal. Calcd for $C_{22}H_{21}NO_5$: C, 69.65; H, 5.58; N, 3.69. Found: C, 69.52; H, 5.68; N, 3.62.

6.4.1.2. 7-Benzoyloxy-4-methyl-8-(4-methylpiperazin-1-yl)methylcoumarin (4b). Mp 141–142 °C; yield 40%. IR (KBr), ν(cm^{-1}): 2936, 2837, 1743, 1726, 1600, 1229. ^{1}H NMR ($CDCl_3$) δ: 1.95–2.26 (m, 7H, CH_3–N–$CH_2$$CH_2$), 2.31–2.59 (m, 7H, 4-$CH_3$, CH_3–N–$CH_2$$CH_2$), 3.82 (s, 2H, CH_2 bridge), 6.33 (s, 1H, H-3), 7.22 (d, J = 8, 1H, H-6), 7.49–8.40 (m, 6H, H-5, H arom.). Anal. Calcd for $C_{23}H_{24}N_2O_4$: C, 70.39; H, 6.16; N, 7.14. Found: C, 70.18; H, 6.19; N, 7.21.

6.4.1.3. 7-Benzoyloxy-8-(tetrahydroisoquinolin-1-yl)-methylcoumarin (4c). Mp 152–154 °C; yield 65%. IR (KBr), ν(cm^{-1}): 2906, 2854, 1733, 1625, 1603, 1244. ^{1}H NMR ($CDCl_3$), δ: 2.55–2.78 (m, 4H, –N–CH_2–CH_2–Ar), 3.55 (s, 2H, –N–CH_2–Ar), 3.95 (s, 2H, CH_2 bridge), 6.45 (d, 1H, J = 10, H-3), 6.80–8.25 (m, 12H, H-4, H-5, H-6, H arom.). Anal. Calcd for $C_{26}H_{21}NO_4$: C, 75.90; H, 5.14; N, 3.40. Found: C, 76.12; H, 5.06; N, 3.38.

6.4.1.4. 7-Benzoyloxy-4methyl-8-(tetrahydroisoquinolin-1-yl)methylcoumarin (4d). Mp 180–182 °C; yield 40%. IR (KBr), ν(cm^{-1}): 2922, 2840, 1738, 1598, 1223. ^{1}H NMR ($CDCl_3$) δ: 2.49 (s, 3H, 4-CH_3), 2.58–2.79 (m, 4H, N–$CH_2$$CH_2$), 3.57 (s, 2H, N–$CH_2$–Ar), 3.99 (s, 2H, CH_2 bridge), 6.36 (s, 1H, H-3), 6.90–8.26 (m, 11H, H-5, H-6, H arom.). Anal. Calcd for $C_{27}H_{23}NO_4$: C, 76.22; H, 5.45; N, 3.29. Found: C, 76.51; H, 5.54; N, 3.19.

6.4.1.5. 7-Benzoyloxy-8-(*trans*-4-cinnamylpiperazin-1-yl)-4-methylcoumarin (4e). Mp 221–223 °C; yield 68%. IR (KBr), ν(cm^{-1}): 2948, 2824, 1732, 1630, 1599, 1235. ^{1}H NMR ($CDCl_3$), δ: 2.49 (s, 3H, 4-CH_3), 2.72–2.95 (m, 8H, –N–CH_2–CH_2–N–), 3.63 (d, J = 5, 2H, –N–CH_2–CH═), 3.97 (s, 2H, CH_2 bridge), 6.25–6.68 (m, 3H, H-3, –CH═CH–), 7.25–8.35 (m, 12H, H-5, H-6, H arom.). ^{13}C NMR ($CDCl_3$), δ: 18.2 (4-CH_3), 48.0 (α N–CH_2), 48.4 (CH_2 bridge), 48.7 (β N–CH_2), 58.0 (CH_2–CH═), 113.8 (C-3), 115.3 (═CH–Ar), 116.8 (C-6), 117.4 (C-8), 118.7 (C-9), 124.2 (C-5), 126.3 (C-2″,6″), 127.9 (C-4″), 128.1 (C-3″,5″), 128.2 (C-3′,5′), 128.3 (C-2′,6′), 129.2 (C-1′), 133.5 (C-4′), 134.0 (C-1″), 139.4 (═CH–CH_2), 151.5 (C-10), 152.1 (C-7), 152.2 (C-4), 159.0 (C-2), 164.3 (CO). Anal. Calcd for $C_{31}H_{30}N_2O_4$: C, 75.28; H, 6.11; N, 5.66. Found: C, 75.51; H, 6.04; N, 5.74.

6.4.1.6. 8-{4-[(1,3-Benzodioxol-5-yl)methyl]piperazin-1-yl}methyl-7-benzoyloxycoumarin (4f). Mp 227–228 °C; yield 56%. IR (KBr), ν(cm^{-1}): 2958, 2837, 1737, 1598,1253. ^{1}H NMR ($CDCl_3$+DMSO-d_6) δ: 2.65–2.88 (m, 8H, N–$CH_2$$CH_2$–N), 3.91 (s, 2H, N–$CH_2$ benzodioxole), 3.98 (s, 2H, CH_2 bridge), 6.06 (s, 2H, O–CH_2–O), 6.46 (d, J = 9, 1H, H-3), 6.85–8.32 (m, 11H, H-4, H-5, H-6, H arom.). Anal. Calcd for $C_{29}H_{26}N_2O_6$: C, 69.87; H, 5.26; N, 5.62. Found: C, 70.10; H, 5.33; N, 5.54.

6.4.1.7. 7-Benzoyloxy-8-[4-(ethoxycarbonyl)piperazin-1-yl]-4-methylcoumarin (4g). Mp 177–178 °C; yield 65%. IR (KBr), ν(cm^{-1}): 2931, 2846, 1742, 1728, 1704, 1600, 1232. ^{1}H NMR ($CDCl_3$) δ: 1.20 (t, J = 7.5, 3H, CH_3–CH_2), 2.12–2.58 (m, 7H, 4-CH_3, CH_2–N–CO), 2.98–

3.29 (m, 4H, CH_2–N–CH_2), 3.86 (s, 2H, CH_2 bridge), 4.11 (q, $J = 7.5$, 2H, O–CH_2), 6.36 (s, 1H, H-3), 7.13–8.42 (m, 7H, H-5, H-6, H arom.). Anal. Calcd for $C_{25}H_{26}N_2O_6$: C, 66.66; H, 5.82; N, 6.22. Found: C, 66.41; H, 5.73; N, 6.28.

6.5. Unsymmetrical derivatives 7

To 5 g of glutaric anhydride, heated until fusion occurred (60 °C), 2.0 mmol (0.26 g) of 2-methylindole was added, then 2.0 mmol of 7-hydroxy-8-piperidinomethylcoumarin (or 7-hydroxy-4-methyl-8-piperidinomethylcoumarin) was added, and the solution was heated at 95 °C for 1.5 h. After cooling, the solution was poured onto crushed ice and the mixture was stirred for 1–2 h. The precipitate was filtered and the solid was crystallized from ethyl acetate. The following compounds were obtained:

6.5.1. Glutaric acid mono 8-[(2′-methylindol-3′-yl)-methyl]coumarin-7-yl ester (7g). Mp 202–203 °C; yield 56%. IR (KBr), ν(cm^{-1}): 3341, 2907 (broad), 1760, 1743, 1722, 1635, 1600. ^{1}H NMR (DMSO-d_6) δ: 2.10–2.81 (m, 9H, CH_3, CH_2), 4.07 (s, 2H, CH_2 bridge), 6.46 (d, $J = 9$, 1H, H-3), 6.80–8.21 (m, 7H, H-4, H-5, H-6, H arom.), 10.88 (s, 1H, NH). Anal. Calcd for $C_{24}H_{21}NO_6$: C, 68.73; H, 5.05; N, 3.34. Found: C, 68.77; H, 4.96; N, 3.27.

6.5.2. Glutaric acid mono 8-[(2′-methylindol-3′-yl)-methyl]-4-methylcoumarin-7-yl ester (7h). Mp 201–202 °C; yield 62%. IR (KBr), ν(cm^{-1}): 3335, 2903 (broad), 1754, 1734, 1716, 1630, 1599. ^{1}H NMR (DMSO-d_6) δ: 2.12–2.68 (m, 12H, CH_3, CH_2), 4.13 (s, 2H, CH_2 bridge), 6.25 (s, 1H, H-3), 6.76–7.72 (m, 6H, H-5, H-6, H arom.), 10.02 (s, 1H, NH). Anal. Calcd for $C_{25}H_{23}NO_6$: C, 69.27; H, 5.35; N, 3.23. Found: C, 69.54; H, 5.40; N, 3.14.

6.6. Biological assays

6.6.1. Compounds. Compounds were dissolved in DMSO at 100 mM and then diluted in culture medium.

6.6.2. Cells and viruses. Cell lines were purchased from American Type Culture Collection (ATCC). The absence of mycoplasma contamination was checked periodically by the Hoechst staining method. Cell lines supporting the multiplication of RNA viruses were the following: Madin Darby Bovine Kidney (MDBK); Baby Hamster Kidney (BHK-21); $CD4^+$ human T-cells containing an integrated HTLV-1 genome (MT-4); Monkey kidney (Vero 76) cells.

6.6.3. Cytotoxicity assays. For cytotoxicity tests, run in parallel with antiviral assays, MDBK, BHK, and Vero 76 cells were resuspended in 96 multiwell plates at an initial density of 6×10^5, 1×10^6, and 5×10^5 cells/ml, respectively, in maintenance medium, without or with serial dilutions of test compounds. Cell viability was determined after 48–120 h at 37 °C in a humidified CO_2 (5%) atmosphere by the MTT method. The cell number of Vero 76 monolayers was determined by staining with the crystal violet dye.

For cytotoxicity evaluations, exponentially growing cells derived from human hematological tumors [$CD4^+$ human T-cells containing an integrated HTLV-1 genome (MT-4)] were seeded at an initial density of 1×10^5 cells/ml in 96-well plates in RPMI-1640 medium supplemented with 10% fetal calf serum (FCS), 100 U/ml penicillin G, and 100 μg/ml streptomycin. Cell cultures were then incubated at 37 °C in a humidified, 5% CO_2 atmosphere in the absence or presence of serial dilutions of test compounds. Cell viability was determined after 96 h at 37 °C by the 3-(4,5-dimethylthiazol-2-yl)-2,5-diphenyl-tetrazolium bromide (MTT) method.[38]

6.6.4. Antiviral assays. Activity of compounds against yellow fever virus (YFV), 17D vaccine strain, was based on inhibition of virus-induced cytopathogenicity in acutely infected BHK-21 cells. Activities against bovine viral diarrhoea virus 1 (BVDV, strain NADL, ATCC Number VR-534), in infected MDBK cells, and against respiratory syncytial virus (RSV), A-2 strain, in infected Vero 76 cells, were also based on inhibition of virus-induced cytopathogenicity.

BHK, MDBK, and Vero 76 cells were seeded in 96-well plates at a density of 5×10^4, 3×10^4, and 2.5×10^4 cells/well, respectively, and were allowed to form confluent monolayers by incubating overnight in growth medium at 37 °C in a humidified CO_2 (5%) atmosphere. Cell monolayers were then infected with 50 μl of a proper virus dilution (in serum-free medium) to give an m.o.i = 0.01 (0.1 in the case of RSV). One hour later, 50 μl of MEM Earle's medium (Dulbecco's modified Eagle's medium for Vero/RSV), supplemented with inactivated fetal calf serum (FCS), 1% final concentration, without or with serial dilutions of test compounds, was added. After a 3-day incubation (5 days for Vero/RSV) at 37 °C, cell viability was determined by the MTT method. In the case of Vero/RSV, cell viability was determined with crystal violet staining of the monolayer (see below), followed by OD determination in spectrophotometer at 570 nm of the dye recovered from the monolayer solubilized with a solution containing 1% sarkosyl and Hepes 10%. 2′-C-Me-guanosine and 6-Aza-Uridine were used as reference compounds for Flaviviridae and RSV, respectively.

6.7. Molecular modeling methods

The starting 3-D model of the HCV RNA-dependent RNA polymerase (RdRp) was based on its X-ray crystallographic structure[39] (chain B, PBD Code: 1CSJ). Missing hydrogen atoms were added to the protein backbone and side chains with the parse module of Amber 7.0.[40,41] All ionizable residues were considered in the standard ionization state at neutral pH. The geometry of added hydrogen was refined for 200 steps (steepest descent) in vacuum, using the well-validated, all-atom force field (FF) parameter set (*parm94*) by Cornell et al.[42] Further protein geometry refinement was carried out using the *sander* module of Amber 7.0 via a combined steepest descent—conjugate gradient algorithm, using the root-mean-square of the Cartesian elements of the gradient equal to 0.01 kcal/(mol Å) as a convergence cri-

terion for the energy gradient. The generalize born/surface area (GB/SA) continuum solvation model[43,44] was used to mimic a water environment. As expected, no relevant structural changes were observed between RdRp relaxed model and the original 3-D structure.

The model structures of the selected inhibitors were generated using Biopolymer module of Insight II (v. 2000.1, Accelrys Inc., San Diego, CA, USA). All molecules were subjected to an initial energy minimization, again using the *sander* module of the Amber 7.0 suite of programs, with the *parm94* version of the Amber force field.[42] In this case, the convergence criterion was set at 10^{-4} kcal/(mol Å). A conformational search was carried out using a well-validated, ad hoc developed combined molecular mechanics/molecular dynamics simulated annealing (MDSA) protocol.[45–48] Accordingly, the relaxed structures were subjected to 5 repeated temperature cycles (from 310 to 1000 K and back) using constant volume/constant temperature (NVT) MD conditions. At the end of each annealing cycle, the structures were again energy minimized to converge below 10^{-4} kcal/(mol Å), and only the structures corresponding to the minimum energy were used for further modeling. The atomic partial charges for the geometrically optimized compounds were obtained using the RESP procedure,[49] and the electrostatic potentials were produced by single-point quantum mechanical calculations at the Hartree–Fock level with a 6-31G* basis set, using the Merz–Singh–Kollman van der Waals parameters.[50,51] Eventual missing force field parameters for the molecules were generated as follows: AM1[52] geometry optimization of the structure was followed by RHF/6-31G* single point calculation to obtain the electrostatic potentials. Next, the RESP method[40] was used for charge fitting. The missing bond, angle torsion, or van der Waals parameters not included in the *parm94* were transferred[53] from the newly developed *parm99* parameter set,[54] or from a general AMBER force field (GAFF).[55]

The optimized structures of the test compounds were docked into the HCV polymerase allosteric binding site by applying a consolidated procedure[46,56,57]; accordingly, it will be described here only briefly. The software AutoDock 3.0[58] was employed to estimate the possible binding orientations of all compounds in the receptor. In order to encase a reasonable region of the protein surface and interior volume, centered on the crystallographic identified binding site, the grids were 60 Å on each side. Grid spacing (0.375 Å), and 120 grid points were applied in each Cartesian direction so as to calculate mass-centered grid maps. Amber 12-6 and 12-10 Lennard–Jones parameters were used in modeling van der Waals interactions and hydrogen bonding (N–H, O–H, and S–H), respectively. In the generation of the electrostatic grid maps, the distance-dependent relative permittivity of Mehler and Solmajer[59] was applied.

For the docking of each compound to the protein, three hundred Monte Carlo/Simulated Annealing (MC/SA) runs were performed, with 100 constant temperature cycles for simulated annealing. For these calculations, the GB/SA implicit water model was again used to mimic the solvated environment. The rotation of the angles ϕ and φ, and the angles of the side chains was set free during the calculations. All other parameters of the MC/SA algorithm were kept as default. Following the docking procedure, the structure of all compounds was subjected to cluster analysis with a tolerance of 1 Å for an all-atom root-mean-square (RMS) deviation from a lower-energy structure representing each cluster family. In the absence of any relevant crystallographic information, the structure of each resulting complex characterized by the lowest interaction energy in the prevailing cluster was selected for further evaluation.

Each best substrate/RdRp complex, resulting from the automated docking procedure, was further refined in the Amber 7.0 suite using the quenched molecular dynamics (QMD) method.[60] In this case, 100 ps MD simulation at 310 K was employed to sample the conformational space of the substrate–enzyme complex in the GB/SA continuum solvation environment. The integration step was equal to 1 fs. After each ps, the system was cooled to 0 K, the structure was extensively minimized, and stored. To prevent global conformational changes of the enzyme, the backbone of the protein binding site was constrained by a harmonic force constant of 100 kcal/Å, whereas the amino acid side chains and the ligands were allowed to move without any constraint.

The best energy configuration of each complex resulting from the previous step was allowed to relax in a 55-Å radius sphere of TIP3P water molecules.[61] The resulting system was minimized with a gradual decrease in the position restraints of the protein atoms. At the end of the relaxation process, all water molecules beyond the first hydration shell (i.e., at a distance >3.5 Å from any protein atom) were removed. Finally, to achieve electroneutrality, a suitable number of counterions were added, in the positions of the largest electrostatic potential, as determined by the *cion* module within Amber 7.0. To reduce computational time to reasonable limits, all protein residues with any atom closer than 20 Å from the center of the mass of each bounded ligand were chosen to be flexible in the dynamic simulations. Subsequently, a spherical TIP3P water cap of radius equal to 20 Å was centered on each inhibitor in the corresponding RdRp complex, including the hydrating water molecules within the sphere resulting from the previous step. After energy minimization of the new water cap for 1500 steps, keeping the protein, the ligand, and the pre-existing waters rigid, followed by a MD equilibration of the entire water sphere with fixed solute for 20 ps, further unfavorable interactions within the structures were relieved by progressively smaller positional restraints on the solute (from 25 to 0 kcal/(mol Å^2)) for a total of 4000 steps. Each system was gradually heated to 310 K at three intervals, allowing a 5 ps interval per each 100 K, and then equilibrated for 50 ps at 310 K, followed by 400 ps of data collection runs, necessary for the estimation of the free energy of binding (vide infra). The MD simulations were performed at constant $T = 310$ K using the Berendsen et al. coupling algorithm[62] with separate

coupling of the solute and solvent to heat, an integration time step of 2 fs, and the applications of the shake algorithm[63] to constrain all bonds to their equilibrium values, thus removing high frequency vibrations. Long-range non-bonded interactions were truncated by using a dual cutoff of 9 and 13 Å, respectively, where energies and forces due to interactions between 9 and 13 Å were updated every 20 time step. The same frequency of update was employed for the non-bonded list. For the calculation of the binding free energy between the RdRp and each compound in water, a total of 400 snapshots were saved during the MD data collection period described above, one snapshot per each 1 ps of MD simulation.

The binding free energy ΔG_{bind} of each RdRp/drug complex in water was calculated according to the procedure termed Molecular Mechanic/Poisson–Boltzmann Surface Area (MM/PBSA), and proposed by Srinivasan et al.[64] Since the theoretical background of this methodology is described in detail in the original papers by Peter Kollman and his group,[65] it will be only briefly described below. Basically, an MD simulation (typically in explicit solvent) is first carried out which yields a representative ensemble of structures. The average total free energy of the system, G, is then evaluated as:

$$\begin{aligned} G &= G_{\text{solv}} + E_{\text{MM}} - \text{TS}_{\text{solute}} \\ &= G_{\text{PB}} + G_{\text{NP}} + E_{\text{MM}} - \text{TS}_{\text{solute}} \end{aligned} \quad (1)$$

in which G_{PB} is the polar solvation energy component, which is calculated in a continuum solvent, usually a finite-difference Poisson–Boltzmann (PB) model, and G_{NP} is the non-polar contribution to the solvation energy, which can be obtained from the solvent accessible surface area (SA). E_{MM} denotes the sum of molecular mechanics (MM) energies of the molecule, and can be further split into contributions from electrostatic (E_{EL}), van der Waals (E_{vdW}), and internal (E_{INT}) energies:

$$E_{\text{MM}} = E_{\text{EL}} + E_{\text{VDW}} + E_{\text{INT}} \quad (2)$$

The last term in Eq. 1, $\text{TS}_{\text{solute}}$, represents the solute entropy, and is usually estimated by a combination of classical statistical formulas and normal-mode analysis.

Using Eqs. 1 and 2, the binding free energy ΔG_{bind} of a given non-covalent association can be obtained as:

$$\Delta G_{\text{bind}} = G_{\text{complex}} - (G_{\text{protein}} + G_{\text{ligand}}) \quad (3)$$

Accordingly, the variation of each contribution to ΔG_{bind} is given by:

$$\Delta E_{\text{MM}} = \Delta E_{\text{EL}} + \Delta E_{\text{VDW}} + \Delta E_{\text{INT}} \quad (4)$$

$$\Delta G_{\text{solv}} = \Delta G_{\text{PB}} + \Delta G_{\text{NP}} \quad (5)$$

The ensemble of structures for the uncomplexed reactants is generated either by running separate MD simulations, or by using the trajectory of the complex, simply by removing the protein or ligand atoms. As reported below, in this work we followed the successful approach proposed by Kuhn and Kollman[66] and applied the latter variant. Accordingly, the term ΔE_{INT} in Eq. 4 is equal to zero. The Poisson–Boltzmann (PB) calculations of ΔG_{PB} were done with the Delphi package,[67] with interior and exterior dielectric constants equal to 1 and 80, respectively. A grid spacing of 2/Å, extending 20% beyond the dimensions of the solute, was employed. The non-polar component ΔG_{NP} was obtained using the following relationship[68]: $\Delta G_{\text{NP}} = \gamma \text{SA} + b$, in which $\gamma = 0.00542$ kcal/(mol Å^2), $b = 0.92$ kcal/mol, and the surface area was estimated by means of the MSMS software.[69] The last parameter in Eq. 1, that is, the change in solute entropy upon association—$T\Delta S_{\text{solute}}$, was calculated through normal-mode analysis.[70] In the first step of this calculation, an 8 Å sphere around the ligand was cut out from an MD snapshot for each ligand–protein complex. This value was shown to be large enough to yield converged mean changes in solute entropy. On the basis of the size-reduced snapshots of the complex, we generated structures of the uncomplexed reactants by removing the atoms of the protein and ligand, respectively. Each of these structures was minimized, using a distance-dependent dielectric constant $\varepsilon = 4r$, to account for solvent screening, and its entropy was calculated using classical statistical formulas and normal-mode-analysis. To minimize the effects due to different conformations adopted by individual snapshots, we averaged the estimation of entropy over 10 snapshots.

Finally, the IC_{50} values were calculated from the corresponding binding free energies using the following relationship[71,72]:

$$\begin{aligned} \Delta G_{\text{bind}} &= RT \ln K_{\text{diss}} = RT \ln(\text{IC}_{50} + 0.50 C_{\text{enz}}) \\ &\cong RT \ln \text{IC}_{50} \end{aligned} \quad (6)$$

The overall quality of the entire procedure described above—that is, protein and inhibitors modeling, conformational analysis, docking and energetic calculations—has been previously tested by carrying out the same calculations on three known RdRp inhibitors,[73,74] for which both the crystallographic structures of the relevant HCV RdRp complexes and the corresponding IC_{50} values were available, and for a new series of nucleoside analogs inhibitors of the HCV RdRp.[75]

Acknowledgment

This work was supported by grants from FIRB 2001 (Italian Foundation for Basic Research).

References and notes

1. Fang, J. W.; Chow, V.; Lau, J. Y. *Clin. Liver Dis.* **1997**, *1*, 493–514.
2. Thomson, B. J.; Finch, R. G. *Clin. Microbiol. Infect.* **2005**, *11*, 86–94.
3. Liang, T. J.; Heller, T. *Gastroenterology* **2004**, *127*(Suppl. 1), S62–S71.
4. Shan, Y.; Chen, X. G.; Huang, B.; Hu, A. B.; Xiao, D.; Guo, Z. M. *Liver Int.* **2005**, *25*, 141–147.

5. Scott, L. J.; Perry, C. M. *Drugs* **2002**, *62*, 507–556.
6. Raptopoulou, M.; Tsantoulas, D.; Vafiadi, I.; Ketikoglou, I.; Paraskevas, E.; Vassiliadis, T.; Kanatakis, S.; Hatzis, G.; Sidiropoulos, L.; Akriviadis, E. *J. Viral Hepat.* **2005**, *12*, 91–95.
7. Pietschmann, T.; Bartenschlager, R. *Curr. Opin. Drug Discov. Dev.* **2001**, *4*, 657–664.
8. Zhong, J.; Gastaminza, P.; Cheng, G.; Kapadia, S.; Kato, T.; Burton, D. R.; Wieland, S. F.; Uprichard, S. L.; Wakita, T.; Chisari, F. V. *Proc. Natl. Acad. Sci. U.S.A.* **2005**, 9294–9299.
9. Lindenbach, B. D.; Evans, M. J.; Syder, A. J.; Wolk, B.; Tellinghuisen, T. L.; Liu, C. C.; Maruyama, T.; Hynes, R. O.; Burton, D. R.; McKeating, J. A.; Rice, C. M. *Science* **2005**, 623–626.
10. Dymock, B. W.; Jones, P. S.; Wilson, F. X. *Antiviral Chem. Chemother.* **2000**, *11*, 79–96.
11. Beaulieu, P. L.; Tsantrizos, Y. S. *Curr. Opin. Invest. Drugs* **2004**, *5*, 838–850.
12. Sulkowski, M. S. *Curr. Gastroenterol. Rep.* **2007**, *9*, 5–13.
13. Toniutto, P.; Fabris, C.; Bitetto, D.; Fornasiere, E.; Rapetti, R.; Pirisi, M. *Discov. Med.* **2007**, *7*, 27–32.
14. Olsen, D. B.; Eldrup, A. B.; Bartholomew, L.; Bhat, B.; Bosserman, M. R.; Ceccacci, A.; Colwell, L. F.; Fay, J. F.; Flores, O. A.; Getty, K. L.; Grobler, J. A.; LaFemina, R. L.; Markel, E. J.; Migliaccio, G.; Prhavc, M.; Stahlhut, M. W.; Tomassini, J. E.; MacCoss, M.; Hazuda, D. J.; Carroll, S. S. *Antimicrob. Agents Chemother.* **2004**, *48*, 3944–3953.
15. Sperandio, D.; Gangloff, A. R.; Litvak, J.; Goldsmith, R.; Hataye, J. M.; Wang, V. R.; Shelton, E. J.; Elrod, K.; Janc, J. W.; Clark, J. M.; Rice, K.; Weinheimer, S.; Yeung, K. S.; Meanwell, N. A.; Hernandez, D.; Staab, A. J.; Venables, B. L.; Spencer, J. R. *Bioorg. Med. Chem. Lett.* **2002**, *12*, 3129–3133.
16. Dhanak, D.; Duffy, K. J.; Johnston, V. K.; Lin-Goerke, J.; Darcy, M.; Shaw, A. N.; Gu, B.; Silverman, C.; Gates, A. T.; Nonnemacher, M. R.; Earnshaw, D. L.; Casper, D. J.; Kaura, A.; Baker, A.; Greenwood, C.; Gutshall, L. L.; Maley, D.; Del Vecchio, A.; Macarron, R.; Hofmann, G. A.; Alnoah, Z.; Cheng, H.-Y.; Chan, G.; Khandekar, S.; Keenan, R. M.; Sarisky, R. T. *J. Biol. Chem.* **2002**, *277*, 38322–38327.
17. Gu, B.; Johnston, V. K.; Gutshall, L. L.; Nguyen, T. T.; Gontarek, R. R.; Darcy, M. G.; Tedesco, R.; Dhanak, D.; Duffy, K. J.; Kao, C. C.; Sarisky, R. T. *J. Biol. Chem.* **2003**, *278*, 16602–16607.
18. Be aulieu, P. L.; Bos, M.; Bousquet, Y.; DeRoy, P.; Fazal, G.; Gauthier, J.; Gillard, J.; Goulet, S.; McKercher, G.; Poupart, M. A.; Valois, S.; Kukolj, G. *Bioorg. Med. Chem. Lett.* **2004**, *14*, 967–971.
19. McKercher, G.; Beaulieu, P. L.; Lamarre, D.; La Plante, S.; Lefebvre, S.; Pellerin, C.; Thauvette, L.; Kukolj, G. *Nucleic Acids Res.* **2004**, *32*, 422–431.
20. Llinas-Brunet, M.; Bailey, M. D.; Bolger, G.; Brochu, C.; Faucher, A. M.; Ferland, J. M.; Garneau, M.; Ghiro, E.; Gorys, V.; Grand-Maitre, C.; Halmos, T.; Lapeyre-Paquette, N.; Liard, F.; Poirier, M.; Rheaume, M.; Tsantrizos, Y. S.; Lamarre, D. *J. Med. Chem.* **2004**, *47*, 1605–1608.
21. Zhang, R.; Durkin, J. P.; Windsor, W. T. *Bioorg. Med. Chem. Lett.* **2002**, *12*, 1005–1008.
22. Soler, M.; McHutchison, J. G.; Kwoh, T. J.; Dorr, F. A.; Pawlotsky, J. M. *Antiviral Ther.* **2004**, *9*, 953–968.
23. Mazzei, M.; Sottofattori, E.; Dondero, R.; Ibrahim, M.; Melloni, E.; Michetti, M. *Il Farmaco* **1999**, *54*, 452–460.
24. Mazzei, M.; Miele, M.; Nieddu, E.; Bruzzo, C.; Barbieri, F.; Alama, A. *Eur. J. Med. Chem.* **2001**, *36*, 915–923.
25. Mazzei, M.; Dondero, R.; Sottofattori, E.; Melloni, E.; Minafra, R. *Eur. J. Med. Chem.* **2001**, *36*, 851–861.
26. Egan, D.; O'Kennedy, E.; Moran, E.; Cox, D.; Prosser, E.; Thornes, R. D. *Drug. Metab. Rev.* **1990**, *22*, 503–529.
27. Kontogiorgis, C. A.; Hadjipavlou-Litina, D. J. *J. Med. Chem.* **2005**, *48*, 6400–6408.
28. Nofal, Z. M.; el-Zahar, M. I.; Abd El-Karim, S. S. *Molecules* **2000**, *5*, 99–113.
29. Galabov, A. S.; Iosifova, T.; Vassileva, E.; Kostova, I. *Z. Naturforsch., C* **1996**, *51*, 558–562.
30. Al-Mawsawi, L. Q.; Fikkert, V.; Dayam, R.; Witvrouw, M., ; Burke, T. R., Jr.; Borchers, C. H.; Neamati, N. *Proc. Natl. Acad. Sci. U.S.A.* **2006**, *103*, 10080–10085.
31. Wu, J.; Yang, Z.; Fathi, R.; Zhu, Q. US Patent 2004180950, 2004, January 06.
32. Xu, B.; Zhu, Q.; Cho, H. J.; Fathi, R.; Yang, Z.; Sandresagra; A., Liu, Y. US Patent 2006223783, 2005, March 29.
33. Okamoto, T.; Kajino, K.; Hino, O. *Jpn. J. Pharmacol.* **2001**, *87*, 177–180.
34. Okamoto, T.; Kobayashi, T.; Yoshida, S. *Curr. Med. Chem. Anticancer Agents* **2005**, *5*, 47–51.
35. Okamoto, T.; Kobayashi, T.; Yoshida, S. *Med. Chem.* **2007**, *3*, 35–44.
36. Mazzei, M.; Miele, M.; Nieddu, E.; Barbieri, F.; Bruzzo, C.; Alama, A. *Eur. J. Med. Chem.* **2001**, *36*, 915–923.
37. Gupta, V. N.; Sharima, B. R.; Avora, R. B. *J. Sci. Ind. Res.* **1961**, *20B*, 300.
38. Pauwels, R.; Balzarini, J.; Baba, M.; Snoeck, R.; Schols, D.; Herdewijn, P.; Desmyster, J.; De Clercq, E. *J. Virol. Methods* **1988**, *20*, 309–321.
39. Bressanelli, S.; Tomei, L.; Rey, F. A.; De Francesco, R. *J. Virol.* **2002**, *76*, 3482–3492.
40. Pearlman, D. A.; Case, D. A.; Caldwell, J. W.; Ross, W. S., ; Cheatham, T. E., III; DeBolt, S.; Ferguson, D.; Seibel, G.; Kollman, P. A. *Comput. Phys. Commun.* **1995**, *91*, 1–41.
41. Case, D. A.; Pearlman, D. A.; Caldwell, J. W., Cheatham, T. E.; Wang, J.; Ross, W. S.; Simmerling, C.; Darden, T. A.; Merz, K. M.; Stanton, R. V.; Cheng, A. L.; Vincent, J. J.; Crowley, M.; Tsui, V.; Gohlke, H.; Radmer, R. J.; Duan, Y.; Pitera, J.; Massova, I.; Seibel, G. L.; Singh, U. C.; Weiner, P. K.; Kollman, P. A. AMBER 7, University of California, San Francisco, CA USA, 2000.
42. Cornell, W. D.; Cieplak, P.; Bayly, C. I.; Gould, I. R.; Merz, K. M.; Ferguson, D. M.; Spellmeyer, D. C.; Fox, T.; Caldwell, J. W.; Kollman, P. A. *J. Am. Chem. Soc.* **1995**, *117*, 5179–5197.
43. Onufriev, A.; Bashford, D.; Case, D. A. *J. Phys. Chem. B* **2000**, *104*, 3712–3720.
44. Feig, M.; Onufriev, A.; Lee, M.; Im, W.; Case, D. A.; Brooks, C. L., III *J. Comput. Chem.* **2004**, *25*, 265–284.
45. Fermeglia, M.; Ferrone, M.; Pricl, S. *Bioorg. Med. Chem.* **2002**, *10*, 2471–2478.
46. Felluga, F.; Pitacco, G.; Valentin, E.; Coslanich, A.; Fermeglia, M.; Ferrone, M.; Pricl, S. *Tetrahedron Asymmetry* **2003**, *14*, 3385–3399.
47. Manfredini, M.; Solaroli, N.; Angusti, A.; Nalin, F.; Durini, E.; Vertuani, S.; Pricl, S.; Ferrone, M.; Spadari, S.; Focher, F.; Verri, A.; De Clercq, E.; Balzarini, J. *Antiviral Chem. Chemother.* **2003**, *14*, 183–194.
48. Metullio, L.; Coslanich, A.; Fermeglia, M.; Ferrone, M.; Fuchs, S.; Paneni, M. S.; Pricl, S. *Biomacromolecules* **2004**, *5*, 1371–1378.
49. Bayly, C. I.; Cieplak, P.; Cornell, W. D.; Kollman, P. A. *J. Phys. Chem.* **1993**, *97*, 10269–10280.
50. Singh, U. C.; Kollman, P. A. *J. Comput. Chem.* **1984**, *5*, 129–145.

51. Besler, B. H.; Merz, K. M.; Kollman, P. A. *J. Comput. Chem.* **1990**, *11*, 431–439.
52. Dewar, M. J. S.; Zoebisch, E. G.; Healy, E. F.; Stewart, J. J. P. *J. Am. Chem. Soc.* **1985**, *107*, 3902–3909.
53. Huo, S.; Wang, J.; Cieplak, P.; Kollman, P. A.; Kuntz, I. D. *J. Med. Chem.* **2002**, *45*, 1412–1419.
54. Wang, J.; Cieplak, P.; Kollman, P. A. *J. Comput. Chem.* **2000**, *21*, 1049–1074.
55. Wang, J.; Wang, W.; Kollman, P. A.; Case, D. A. *J. Comput. Chem.* **2005**, *25*, 1157–1174.
56. Felluga, F.; Fermeglia, M.; Ferrone, M.; Pitacco, G.; Pricl, S.; Valentin, E. *Tetrahedron Asymmetry* **2002**, *13*, 475–489.
57. Mamolo, M. G.; Zampieri, D.; Vio, L.; Fermeglia, M.; Ferrone, M.; Pricl, S.; Scialino, G.; Banfi, E. *Bioorg. Med. Chem.* **2005**, *13*, 3797–3809.
58. Morris, G. M.; Goodsell, D. S.; Halliday, R. S.; Huey, R.; Hart, W. E.; Belew, R. K.; Olson, A. J. *J. Comput. Chem.* **1998**, *19*, 1639–1662.
59. Mehler, E. L.; Solmajer, T. *Protein Eng.* **1991**, *4*, 903–910.
60. Frecer, V.; Kabelac, M.; De Nardi, P.; Pricl, S.; Miertus, S. *J. Mol. Graphics Modell.* **2004**, *22*, 209–220.
61. Jorgensen, W. L.; Chandrasekhar, J.; Madura, J. D.; Impey, R. W.; Klein, M. L. *J. Chem. Phys.* **1983**, *79*, 926–935.
62. Berendsen, H. J. C.; Postma, J. P. M.; van Gunsteren, W. F.; Di Nola, A.; Haak, J. R. *J. Comput. Phys.* **1984**, *81*, 3684–3690.
63. Ryckaert, J. P.; Ciccotti, G.; Berendsen, H. J. C. *J. Comput. Phys.* **1977**, *23*, 327–341.
64. Srinivasan, J.; Cheatham, T. E., III; Cieplak, P.; Kollman, P. A.; Case, D. A. *J. Am. Chem. Soc.* **1998**, *120*, 9401–9409.
65. Kollman, P. A.; Massova, I.; Reyes, C.; Kuhn, B.; Huo, S.; Chong, L.; Lee, M.; Lee, T.; Duan, Y.; Wang, W.; Donini, O., ; Cieplak, P.; Srinivasan, J.; Case, D. A.; Cheatham, T. E., III *Acc. Chem. Res.* **2000**, *33*, 889–897.
66. Kuhn, B.; Kollman, P. A. *J. Med. Chem.* **2000**, *43*, 3786–3791.
67. Gilson, M. K.; Sharp, K. A.; Honig, B. H. *J. Comput. Chem.* **1987**, *9*, 327–335.
68. Sitkoff, D.; Sharp, K. A.; Honig, B. H. *J. Phys. Chem.* **1994**, *98*, 1978–1988.
69. Sanner, M. F.; Olson, A. J.; Spehner, J. C. *Biopolymers* **1996**, *38*, 305–320.
70. Case, D. A. *Curr. Opin. Struct. Biol.* **1994**, *4*, 285–290.
71. Kroeger Smith, M. B.; Lamb, M. L.; Tirado-Rives, J.; Jorgensen, W. L.; Michejda, C. J.; Ruby, S. K.; Smith, R. H., III *Protein Eng.* **2000**, *13*, 413–421.
72. Wang, J.; Morin, P.; Wang, W.; Kollman, P. A. *J. Am. Chem. Soc.* **2001**, *123*, 5221–5230.
73. Wang, M.; Ng, K. K.; Cherney, M. M.; Chan, L.; Yannopoulos, C. G.; Bedard, J.; Morin, N.; Nguyen-Ba, N.; Alaoui-Ismaili, M. H.; Bethell, R. C.; James, M. N. *J. Biol. Chem.* **2003**, *278*, 9489–9495.
74. Love, R. A.; Parge, H. E.; Yu, X.; Hickey, M. J.; Diehl, W.; Gao, J.; Wriggers, H.; Ekker, A.; Wang, L.; Thomson, J. A.; Dragovich, P. S.; Fuhrman, S. A. *J. Virol.* **2003**, *77*, 7575–7581.
75. Pricl, S.; Manfredini, S.; Angusti, A.; Ciliberti, N.; Durini, E.; Vertuani, S.; Buzzoni, L.; Coslanich, A.; Ferrone, M.; Fermeglia, M.; Paneni, M. S.; La Colla, P.; Sanna, G.; Cadeddu, A.; Mura, M.; Loddo, R. Hindered Nucleoside Analogs as Inhibitors of HCV RNA-Dependent RNA-Polymerase: Evolving Vistas. In *Framing the Knowledge of Viral Hepatitis*; Schinazi, R. F., Schiff, E. R., Eds.; IHL Press: Cambridge MA, USA, 2005; pp 279–318, ISBN: 978-0-9754188-1-9.